

Integrated turnkey soliton microcombs operated at CMOS frequencies

Boqiang Shen^{1,†}, Lin Chang^{2,†,*}, Junqiu Liu^{3,†}, Heming Wang^{1,†}, Qi-Fan Yang^{1,†},
Chao Xiang², Rui Ning Wang³, Jijun He³, Tianyi Liu³, Weiqiang Xie²,
Joel Guo², David Kinghorn², Lue Wu¹, Qing-Xin Ji^{1,4},
Tobias J. Kippenberg^{3,*}, Kerry Vahala^{1,*} and John E. Bowers²

¹T. J. Watson Laboratory of Applied Physics, California Institute of Technology, Pasadena, CA 91125, USA

²ECE Department, University of California Santa Barbara, Santa Barbara, CA 93106, USA

³Institute of Physics, Swiss Federal Institute of Technology Lausanne (EPFL), CH-1015 Lausanne, Switzerland

⁴School of Physics, Peking University, Beijing 100871, China

[†]These authors contributed equally to this work.

*linchang@ucsb.edu, tobias.kippenberg@epfl.ch, vahala@caltech.edu

Abstract: We experimentally discovered and theoretically explain a novel turnkey regime for operation of soliton microcombs, wherein a new operating point enables the direct access of the soliton state by simple turn-on of the pump laser. © 2020 The Author(s)

OCIS codes: (130.3120) Integrated optics devices; (140.3945) Microcavities; (190.0190) Nonlinear optics

Optical frequency combs have found a remarkably wide range of applications in science and technology. And a recent development that portends a revolution in miniature and integrated comb systems is dissipative Kerr soliton formation in coherently pumped high-quality-factor (high-Q) optical microresonators [1]. Also, the recent integration of microresonators with lasers has revealed the viability of fully chip-based soliton microcombs [2, 3]. However, their operation requires complex startup and feedback protocols that necessitate difficult-to-integrate optical and electrical components. Here, a regime for turnkey operation of soliton microcombs co-integrated with a pump laser is demonstrated and theoretically explained. Significantly, a new operating point is shown to appear from which solitons are generated through binary turn-on and turn-off of the pump laser, thereby eliminating all photonic/electronic control circuitry. These features offer compelling advantages for high-volume production.

In the experiment, integrated soliton microcombs whose fabrication and repetition rate are compatible with CMOS circuits are butt-coupled to a commercial distributed-feedback (DFB) laser via inverse tapers (Fig. 1a). The microresonators are fabricated using the photonic Damascene reflow process [4] and feature Q factors exceeding 16 million, resulting in a low milliwatt-level parametric oscillation threshold. Up to 30 mW of optical power is launched into the microresonator. Given its compact footprint and the absence of control electronics, the pump-laser/microcomb chip set was mounted into a butterfly package (Fig. 1b) to facilitate measurements and also enable portability. Fig. 1c shows spectra of multi-soliton states produced by the laser/microcomb chips with 20 GHz and 15 GHz repetition rates. The coherent nature of these soliton microcombs is confirmed by photodetection of the soliton pulse streams, and reveals high-contrast, single-tone electrical signals at the indicated repetition rates.

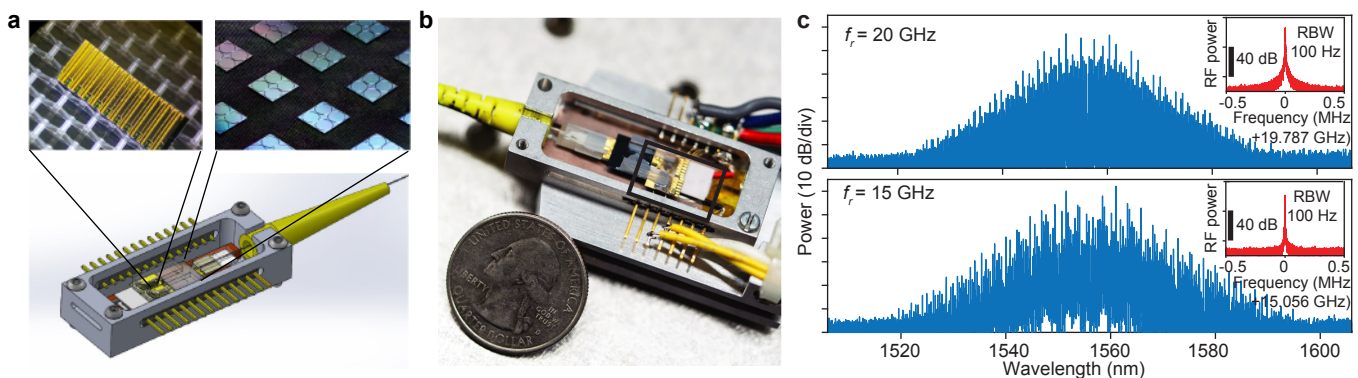


Fig. 1: Integrated soliton microcomb chip and soliton spectrum. (a) Rendering of the soliton microcomb chip that produces soliton pulse signals. Zoom-in panel: Images of a chip of 10 DFB lasers and Si_3N_4 microresonator chip devices. (b) Image of a pump/microcomb in a compact butterfly package. (c) Optical spectra of multi-soliton states at 20 GHz and 15 GHz repetition rates. Insets: Electrical beatnotes showing the repetition rates.

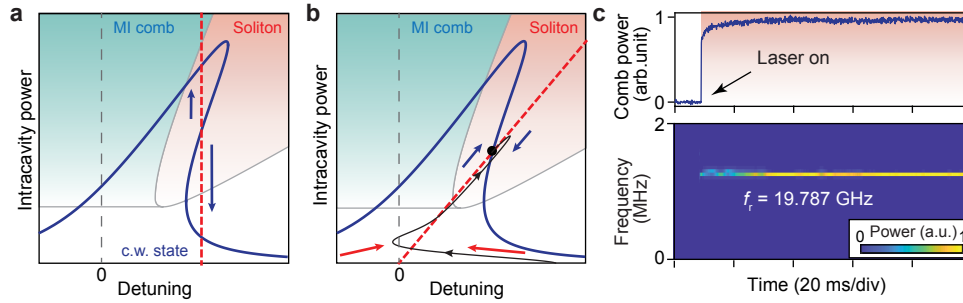


Fig. 2: Turnkey soliton microcomb operation. (a) Phase diagram, hysteresis curve and dynamics of the conventional pumping system. The blue curve is the intracavity power as a function of cavity-pump frequency detuning. Laser tuning (dashed red) accesses multiple equilibria (middle point is unstable as indicated by blue arrows). (b) Phase diagram, hysteresis curve and dynamics of the new pumping system. A modified laser tuning curve (dashed red) intersects the intracavity power curve (blue) to establish a new operating point from which solitons form. The feedback phase ϕ is set to 0 in the plot. Solid black curve is the simulated evolution upon turning-on of the laser at a red detuning outside the soliton regime but within the locking bandwidth. (c) Measured comb power (upper panel) and detected soliton repetition rate signal (lower panel) with laser turn-on indicated at 10 ms.

In conventional pumping of microcombs, the laser is optically-isolated. Intracavity power as a function of pump-cavity detuning features a Kerr-effect bistability. And dynamics can be described using a phase diagram comprising continuous-wave (c.w.), modulation instability (MI) and soliton regimes that are accessed as the pump frequency is tuned across a cavity resonance (Fig. 2a). Tuning through the MI regime seeds the formation of soliton pulses. On account of the thermal hysteresis and the abrupt intracavity power discontinuity upon transition to the soliton regime, special tuning or active capture techniques are required to compensate thermal transients.

Now consider removing the optical isolation so that backscatter feedback occurs from pumping a resonator mode. In prior work semiconductor laser locking to the resonator mode as well as laser line narrowing have been shown to result from backscattering of the intracavity optical field. These attributes as well as mode selection when using a broadband pump have also been profitably applied to operate microcomb systems without isolation [2, 3, 5, 6]. However, these prior studies of feedback effects have considered the resonator to be linear so that the detuning between the feedback-locked laser and the cavity resonance is determined solely by the phase ϕ accumulated in the feedback path [7]. In contrast, here the nonlinear behavior of the microresonator is included and is shown to have a dramatic effect on the system operating point. The relationship between the laser-cavity detuning $\delta\omega$ and intracavity power of the pump mode P_0 can be shown to be approximately given by,

$$\frac{\delta\omega}{\kappa/2} = \tan \frac{\phi}{2} + \frac{3}{2} \frac{P_0}{P_{th}} \quad (1)$$

where κ is the resonance power decay rate and P_{th} is the parametric oscillation threshold for intracavity power. A single operating point at the intersection of Eq. (1) and the soliton hysteresis occurs as shown in Fig. 2b. Control of feedback phase shifts the x-intercept of Eq. (1) to adjust the operating point. The system converges to this equilibrium once the laser frequency is within a locking bandwidth. As verified both numerically (Fig. 2b) and experimentally (Fig. 2c), this behavior enables soliton mode locking by simple power-on of the pump laser (i.e., no triggering or complex tuning schemes). Indeed, the measured comb power shows that a steady soliton power plateau is reached immediately after turn-on of the laser. And the stable soliton emission is further confirmed by monitoring the real-time evolution of the soliton repetition rate signal (Fig. 2c). Finally, the system is observed to be robust with respect to temperature and environmental disturbances.

This work is supported by the Defense Advanced Research Projects Agency, DARPA (HR0011-15-C-055).

References

1. T. J. Kippenberg, A. L. Gaeta, M. Lipson, and M. L. Gorodetsky, *Science* **361** (2018).
2. B. Stern, X. Ji, Y. Okawachi, A. L. Gaeta, and M. Lipson, *Nature* **562**, 401 (2018).
3. A. S. Raja, A. S. Voloshin, H. Guo, S. E. Agafonova, J. Liu *et al.*, *Nat. Commun.* **10**, 680 (2019).
4. J. Liu, A. S. Raja, M. Karpov, B. Ghadiani, M. H. Pfeiffer *et al.*, *Optica* **5**, 1347–1353 (2018).
5. W. Liang, D. Eliyahu, V. Ilchenko, A. Savchenkov, A. Matsko *et al.*, *Nat. Commun.* **6**, 7957 (2015).
6. N. Pavlov, S. Koptyaev, G. Lihachev, A. Voloshin, A. Gorodnitskiy *et al.*, *Nat. Photon.* **12**, 694 (2018).
7. N. Kondratiev, V. Lobanov, A. Cherenkov, A. Voloshin, *et al.*, *Opt. Express* **25**, 28167–28178 (2017).